ELSEVIER

Journal of Alloys and Compounds 279 (1998) 179–183

Journal of ALLOYS AND COMPOUNDS

Unit cell parameters and densities of the gadolinium dihydride GdH_{2+x}

M. Ellner*, H. Reule, E.J. Mittemeijer

Max-Planck-Institut für Metallforschung, Seestraße 92, D-70174 Stuttgart, Germany

Received 22 May 1998

Abstract

Unit cell parameters and macroscopic densities were measured for gadolinium-rich ($x_H<2/3$) and hydrogen-rich compositions ($x_H>2/3$) of the dihydride GdH_{2+x} (defect CaF_2 type). The experimentally determined values of the number of atoms in the unit cell are consistent with the results of earlier work on some dihydrides REH_{2+x} isotypical with CaF_2. It was concluded that for the hydrogen-rich compositions, the excess hydrogen atoms occupy the Wyckoff (octahedral) position (*b*) of the space group $Fm\bar{3}m$, whereas for the gadolinium-rich compositions vacancies occur on the hydrogen sites (*c*). The gadolinium sites (*a*) remain occupied fully by gadolinium atoms in the homogeneity range of the gadolinium dihydride. A set of powder diffraction data was obtained for GdH_2. © 1998 Elsevier Science S.A. All rights reserved.

Keywords: Rare earth elements dihydrides; Defect structures; CaF_2 type representatives

1. Introduction

The incomplete phase diagram of the binary system Gd–H shows a large solubility of hydrogen in α-Gd (Mg type) (up to hydrogen mole fraction $x_H=0.35$ at 1275 K) and two intermediate phases: the dihydride GdH_2 ($0.64<x_H<0.70$, below 875 K) and the trihydride GdH_3 ($0.74<x_H<0.75$, below 875 K) [1]. The structure of GdH_2 is isotypic with CaF_2 (Pearson code *cF*12, space group $Fm\bar{3}m$, $a=5.303$ Å) [2].

A linear increase of the GdH_{2+x} unit cell parameter with temperature was observed for the compositions $0.667<x_H<0.686$ in the temperature range 90 K $< T <$300 K [3]. The high-temperature X-ray measurements of the GdH_{2+x} unit cell parameter showed linearity up to 525 K; a deviation from the linear dependence was observed in the temperature range 550 K–775 K [4]. On the other hand, a non-linear dependence of the unit cell parameter on temperature was measured for compositions $Gd_{31.1}H_{68.9}$ and $Gd_{30.8}H_{69.2}$ [3].

The unit cell parameter of GdH_{2+x}, as measured at room-tempereature, decreases linearly with increasing hydrogen content; but at 90 K a change in the slope $\Delta a/\Delta x_H$ occurs at the hydrogen-rich compositions $Gd_{31.1}H_{68.9}$ and $Gd_{30.8}H_{69.2}$ [3]. Neither density nor powder diffraction data have been reported for the dihydride GdH_{2+x} in the literature [5,6].

This study has been made as a part of an investigation on the structural effects of interstitially dissolved elements, like hydrogen, boron, carbon and nitrogen in transition metals, rare earth metals and their alloys.

2. Experimental

The GdH_{2+x} compounds were prepared starting from gadolinium (purity 99.9%; Rhône–Poulenc). Bulk gadolinium ingots were hydrogenated by exposing them to an H_2 atmosphere (99.999%; Messer Griesheim) of 0.13 MPa at 775 K for 16 hours which yielded the composition $GdH_{2.26(6)}$. Another compound of composition $GdH_{1.93(6)}$ was prepared by partial desorption of a $GdH_{2.26(6)}$ sample in high vacuum. The hydrogen concentration of the samples was determined by means of a desorption method as follows [7]. The samples are placed in a high vacuum system which can be heated up to 975 K at the position of the sample using a radiation furnace. The vacuum system is operated by a turbo molecular pump having a constant pumping rate at pressures between 10^{-9} and 10^{-2} Pa. Hydrogen desorbs from the sample and is detected by a computer controlled mass spectrometer. A calibration of this device showed that the hydrogen concentration can be determined with a maximum relative error of 3%.

---

*Corresponding author.

PII: S0925-8388(98)00681-1

Bulk specimens were ground in a mortar and passed through a sieve (mesh size: 0.05 mm); the particles which passed the sieve were used for the powder diffraction analysis. Powder diffraction patterns were recorded in a Guinier transmission camera (Enraf–Nonius FR552) using Cu $K_{\alpha 1}$ (λ=1.540562 Å) and/or Mo $K_{\alpha 1}$ (λ=0.70930 Å) radiation. Silicon (99.9999999%; Ventron) was used as an internal calibration standard. The powdered specimens were put on a piece of adhesive band and were protected by a fine collodion film to prevent sample decomposition by atmospheric humidity. For comparison, diffraction measurements were also made using the airtight Guinier capillary technique. Both protection methods yielded powder diffraction patterns of the gadolinium dihydride. Single coated CEA Reflex 15 film was used for the Guinier photographs. The unit cell parameter was refined by least squares fitting of Bragg's equation to diffraction lines in the range $29° < 2\theta < 61°$. Integrated intensities of diffraction lines recorded in the Guinier patterns were densitometrically analysed on the Line Scanner LS 20 (KEJ Instruments).

The density of GdH_{2+x} was measured by means of a gas pycnometer ACCUPYC 1330 (Micromeritics Instrument Corporation) using helium (99.999%; Messer Griesheim) as gas medium.

3. Results

Guinier patterns of the $GdH_{1.93(6)}$ specimen showed diffraction lines of the CaF_2 type structure (*Fm*$\bar{3}$*m*, *cF*12). The unit cell parameter *a* of $GdH_{1.93(6)}$ (x_H=0.659(7)<2/3; Cu $K_{\alpha 1}$ radiation, silicon calibration) equals 5.303(1) Å. The density D_m was determined as 7.07 Mg m^{-3}.

Similarly, for the hydrogen-rich composition $GdH_{2.26(6)}$ (x_H=0.693(7)>2/3; Cu $K_{\alpha 1}$ radiation, silicon calibration) the following results were obtained: a=5.284(1) Å, D_m= 7.09 Mg m^{-3}. Hence, with increasing hydrogen content, the unit cell parameter decreases and the density increases.

To produce a comprehensive set of powder diffraction data for GdH_2, Guinier patterns were also recorded with Mo $K_{\alpha 1}$ radiation to have access to lattice spacings, d_o, corresponding to the range of $34° < \theta < 62°$. Powder diffraction data thus determined for $GdH_{1.93(6)}$ have been given in Table 1. For calculation of the powder diffraction intensities, I_c, the program LAZY-PULVERIX was used [8].

Table 1
Powder diffraction data for the dihydride GdH_2

hkl	d_c (Å)	d_o (Å)	I_o	I_c
111	3.0617	3.066	100	100
002	2.6515	2.651	51	49
022	1.8749	1.875	43	38
113	1.5989	1.5989	50	44
222	1.5308	1.5306	11	12
004	1.3258	1.3257	4	6
133	1.2166	1.2161	18	16
024	1.1858	1.1852	11	14
224	1.0825	1.0824	10	10
333	1.0206	1.0203	9	3
115	1.0206	1.0203	9	8
044	0.9374	0.9365	2	3
135	0.8964	0.8960	8	9
244	0.8838	0.8833	3	4
026	0.8385	0.8388	2	3
335	0.8087	0.8088	1	3
226	0.7995	0.7995	1	3
155	0.7426	0.7424	2	2
117	0.7426	0.7424	2	2
046	0.7354	0.7350	1	2
246	0.7086	0.7084	3	3
355	0.6904	0.6904	2	1
137				2

4. Discussion

Many crystalline dihydrides of early transition elements, as well as of rare earth elements and actinides, exhibit the CaF_2 structure. Compared with the CaF_2-isotypical intermetallic compounds (*eg*. $AuAl_2$, $PtAl_2$ [9]), the dihydrides of the rare earth elements show a relatively large homogeneity range, especially at higher temperatures [1]. This region of solid solution formation ranges at high temperature from the rare earth element-rich side (x_H<2/3) up to the hydrogen-rich side (x_H>2/3) of the phase diagram. At low temperatures the region of homogeneity ranges from the stoichiometric composition (x_H=2/3) up to hydrogen-rich compositions. Similar remarks can be made for the 4d-element containing binary system Y–H. In the 3d-element containing binary system Sc–H, the hydrogen-rich phase boundary of ScH_2 is not sufficiently known yet. The scandium-rich phase boundary extends up to x_H~0.5 at a temperature of 1400 K [1].

4.1. Unit cell parameter of RE-dihydrides as function of atomic number

The unit cell parameters of the rare earth element dihydrides (REH_2) as well as of the dihydrides ScH_2 and YH_2 are shown, for the stoichiometrical composition, x_H= 2/3, in Fig. 1 (data from Ref. [10]). Corresponding promethium and europium dihydrides of structure type CaF_2 are unknown. Clearly, for the rare earth elements, the unit cell parameter decreases with increasing atomic number. A similar observation concerning the increase of the X-ray density of some REH_2 with atomic mass as well as the decrease of the interatomic bond length, $d_{RE\text{-}H}$, with atomic mass was reported in Ref. [4]. The decrease of the unit cell parameter *a* with atomic number may be understood recognizing that the atomic radius of the rare earth elements, r_{Re}, decreases with atomic number (i.e. also with atomic mass).

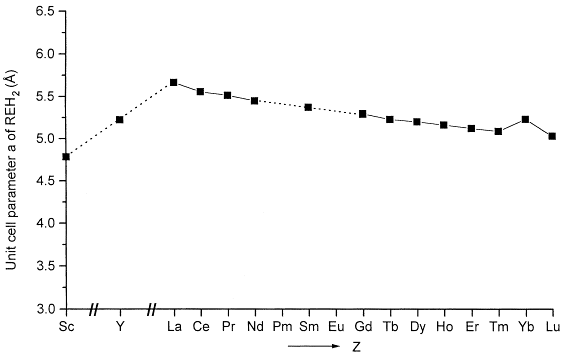

Fig. 1. Unit cell parameter a of the dihydrides ScH_2, YH_2 and REH_2 (RE=rare earth element) as function of the atomic number Z (data from Ref. [10]).

An exception is observed for the dihydride YbH_2 showing a unit cell parameter significantly larger than that of the 'neighbouring' dihydrides, TmH_2 and LuH_2 (r_{Tm}= 1.746 Å and r_{Lu}=1.734 Å; data according to Ref. [11]). Within this context it is remarked that two atomic radii have been reported for ytterbium in Ref. [11]: r_{Yb}=1.940 Å for the bivalent ytterbium, and r'_{Yb}=1.749 Å for the trivalent ytterbium. Hence, it is suggested that bivalent ytterbium occurs in the dihydride YbH_2.

Considering the dihydrides of the 3d-element scandium and the 4d-element yttrium, the unit cell parameter increases with atomic number (Fig. 1) as an immediate consequence of the corresponding increase of the atomic radius (r_{Sc}=1.641 Å and r_Y=1.801 Å [11]).

4.2. Lattice parameter and density of the dihydride GdH_{2+x} as function of hydrogen content

The observation that the GdH_{2+x} unit cell parameter decreases with increasing hydrogen content [3] is confirmed by the measurements presented in Section 3. Comparing the diffraction lines of both specimens, $GdH_{1.93(6)}$ ($x_H<2/3$) and $GdH_{2.26(6)}$ ($x_H>2/3$), the diffraction lines of the hydrogen-rich specimen ($x_H>2/3$) are significantly more diffuse. Similar observations were made before for the dihydrides LaH_{2+x}, CeH_{2+x}, NdH_{2+x}, LaH_{2+x}, CeH_{2+x}, PrH_{2+x} and NdH_{2+x} [12–14].

The average atomic volume V^A is shown as function of the mole fraction x_H in Fig. 2 for the system gadolinium–hydrogen. The following structure data were taken into consideration for this plot: Gd (Mg type) [15], GdH_{2+x} (CaF_2 type, data from this study; Section 3), GdH_3 (HoH_3, anti-Cu_3As type) [16,17] and solid H (Mg type) [18]. Clearly, the average atomic volumes of GdH_{2+x} and GdH_3 are much smaller than those corresponding to a mechanical mixture of gadolinium and solid hydrogen. This may be related to the high negative values of the enthalpy of formation measured for the rare earth element containing dihydrides [19]. Measurements of the unit cell parameter as function of the hydrogen mole fraction ($0.64<x_H<0.73$) reported for LaH_{2+x}, PrH_{2+x}, NdH_{2+x} [13] and for CeH_{2+x} [14] show also a relatively strong negative slope $\Delta a/\Delta x_H$ in the composition range $0.667<x_H<0.706$ for LaH_{2+x}, PrH_{2+x}, NdH_{2+x} and, in the composition range $0.667<x_H<0.697$, for CeH_{2+x}.

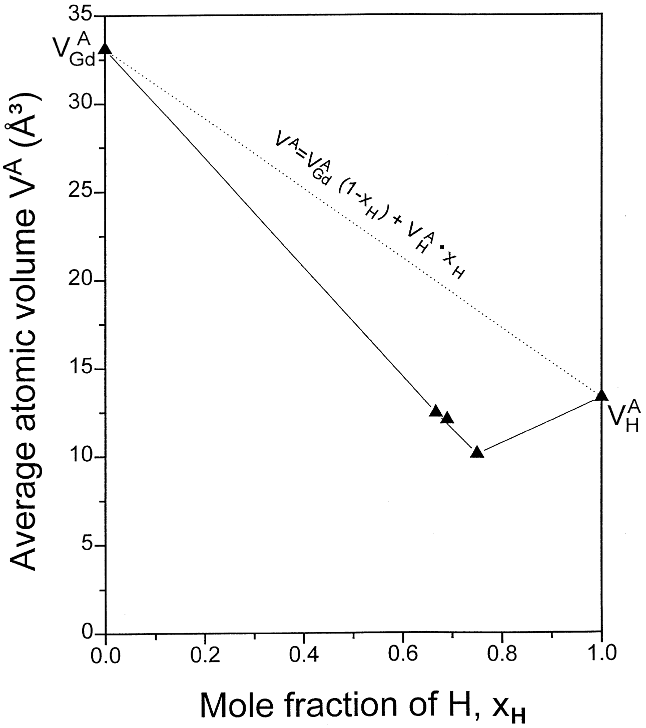

Fig. 2. The average atomic volume, V^A, as function of the mole fraction of hydrogen, x_H, for the binary system Gd–H. Data presented correspond to Gd [15], GdH_{2+x} (see Section 3), GdH_3 [16] and solid H [18].

The number of atoms in the unit cell can be calculated straight forwardly from the unit cell volume, the density and the composition. Thus, using the data obtained in this work, the dependence of the number of atoms in the unit cell of GdH_{2+x}, N^C_A, is shown as function of the mole fraction, x_H, in Fig. 3. Now consider the unit cell of the stoichiometric GdH_2 ($cF12$, CaF_2 type). The space group is $Fm\bar{3}m$ (Nr. 225) and the atomic positions of both components are: 4Gd (a) 0,0,0; 8H (c) 1/4,1/4,1/4; 1/4,1/4,3/4 [20]. The lattice points of the CaF_2 structure are shown in Fig. 4, additional with the lattice point 1/2,1/2,1/2 of the Wyckoff position (b), showing the multiplicity 4. Referring to the Wyckoff position (a) occupied by gadolinium, the Wyckoff position (b) is an octahedral position.

Three kinds of the mole fraction dependence of the number of atoms in the CaF_2 unit cell are shown in Fig. 3:

(i) For the case of complete substitution of hydrogen by gadolinium ($x_H<2/3$) and gadolinium by hydrogen ($x_H>2/3$): $N^C_A=12$ (horizontal dotted line in Fig. 3).

(ii) For the case of filling of the octahedral Wyckoff

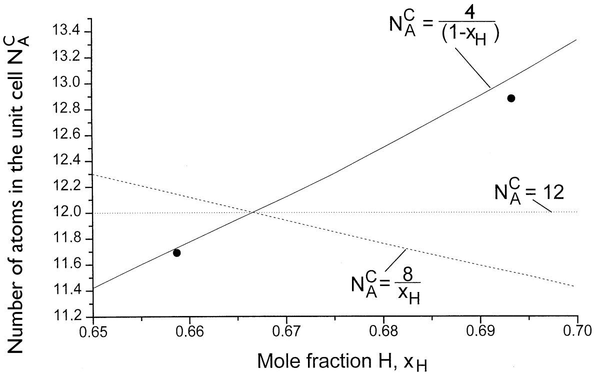

Fig. 3. The number of atoms in the GdH_{2+x} unit cell, N_A^C, as function of the mole fraction of hydrogen, x_H, (i) for the case of substitution of hydrogen by gadolinium for $x_H<2/3$ and gadolinium by hydrogen for $x_H>2/3$: $N_A^C=12$ (horizontal dotted line); (ii) for the case of occupation of the lattice sites (*b*) (Fig. 4) by hydrogen for $x_H>2/3$ and vacancies on the hydrogen lattice sites (*c*) (Fig. 3) for $x_H<2/3$: $N_A^C=4/(1-x_H)$ (full line); (iii) for the case of occupation of lattice sites (*b*) (Fig. 4) by gadolinium for $x_H<2/3$ and vacancies on the lattice sites (*a*) for $x_H>2/3$: $N_A^C=8/x_H$ (dashed line).

position (*b*) by hydrogen ($x_H>2/3$) and for the case of vacancies in the Wyckoff position (*c*) occupied by hydrogen ($x_H<2/3$): $N_A^C=4/(1-x_H)$, (i.e. the partial structure of hydrogen is defective; see full line in Fig. 3).[1]

(iii) For the case of vacancies in the Wyckoff position (*a*) occupied by gadolinium ($x_H>2/3$) and filling of the octahedral position (*b*) by gadolinium ($x_H<2/3$): $N_A^C=8/x_H$ (i.e. the partial structure of gadolinium is defective; see dashed line in Fig. 3).[2]

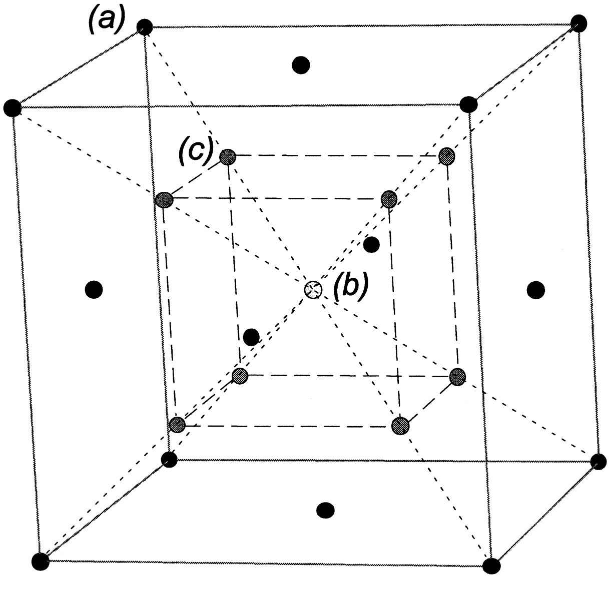

Fig. 4. Lattice points of the CaF_2 structure (space group $Fm\bar{3}m$). The additional lattice point 1/2, 1/2, 1/2 of the Wyckoff position (*b*), showing the multiplicity 4, has been indicated.

As follows from the experimental data of this study ($N_A^C=11.69$ for $GdH_{1.93(6)}$ and $N_A^C=12.88$ for $GdH_{2.26(6)}$) and the calculated curves in Fig. 3, the compositional variation in the GdH_2 structure is realised by maintaining of a full occupation of the atomic position (*a*) by gadolinium, while for $x_H>2/3$ the hydrogen atoms are positioned in the octahedral position (*b*), as also suggested earlier by the neutron diffraction data [12], and for $x_H<2/3$ vacancies occur at the hydrogen lattice sites (*c*) (see full line in Fig. 3).

It is striking to note that the occupation of the octahedral position by excess hydrogen in GdH_2 is accompanied with a *decrease* of the lattice parameter. From a topological point of view this is difficult to understand. In this context reference can be made to earlier work [9] on $PtAl_2$ that also is of CaF_2 structure type. In that case excess aluminium occupies also the octahedral position (*b*), but this is associated with an increase of the lattice parameter [9]. Apparently the type of bonding is rather different for GdH_2 and $PtAl_2$. This is also suggested by the different enthalpies of formation: −86 kJ/g-atom for $PtAl_2$ [21] and of the order of −200 kJ/g-atom for the dihydrides of the rare earth elements [22].

An attempt to explain the anomalous decrease of the unit cell parameters with increasing occupation of the octahedral positions (*b*) by hydrogen involved assumption of a change in bonding upon increasing x_H in REH_{2+x} phases was made earlier [14]: instead of the preferred bonding RE–RE for $x_H\leq 2/3$, the bonding RE–H becomes relatively significant for $x_H>2/3$.

5. Conclusions

(i) The unit cell volume of the rare earth element dihydrides (REH_2) decreases with the atomic number of RE, reflecting a corresponding decrease of the atomic radius of RE.

(ii) The unit cell volume of GdH_{2+x} decreases with increasing hydrogen content, while the density of GdH_{2+x} increases with increasing hydrogen content.

(iii) Compositional variation in GdH_{2+x} (defect CaF_2 structure, space group $Fm\bar{3}m$) is realized by hydrogen atom occupation of the octahedral interstitial positions (*b*) (for $x_H>2/3$) and by vacancies on the atomic positions (c) occupied by hydrogen (for $x_H<2/3$). The gadolinium sites (*a*) remain occupied fully by gadolinium atoms (both for $x_H\leq 2/3$ and for $x_H>2/3$).

---

[1] Number of atoms in unit cell$=N_A^C=4Gd+8H-\beta H$ vacancies on sites $(c)+\alpha H$ on sites $(b)=12+(\alpha-\beta)$. As $x_H=\{8+(\alpha-\beta)\}/\{12+(\alpha-\beta)\}$, it straight forwardly follows $N_A^C=4/(1-x_H)$.

[2] Number of atoms in unit cell$=N_A^C=4Gd-\gamma Gd$ vacancies on sites $(a)+\delta Gd$ on sites $(b)+8H=12+(\delta-\gamma)$. As $x_H=8/\{12+(\gamma-\delta)\}$ it follows: $N_A^C=8/x_H$.

References

[1] T. Massalski, H. Okamoto, P.R. Subramanian, L. Kacprzak, Binary Alloys Phase Diagrams, Second Edition, ASM International, The Materials Information Society, 1990.
[2] G.R. Sturdy, R.N.R. Mulford, J. Am. Chem. Soc. 78 (1956) 1083.
[3] M. Chiheb, J.N. Daou, P. Vajda, Z. Phys. Chemie 179 (1993) 255.
[4] J.E. Bonnet, J.N. Daou, J. Appl. Physics 48 (1977) 964.
[5] P. Villars, Pearson's Handbook, Desk Edition, Crystallographic Data for Intermetallic Phases, ASM International, The Materials Information Society, Materials Park, OH, 1997.
[6] Powder Diffraction File (Sets 1-47), International Centre for Diffraction Data, Newtown Square, Pennsylvania, USA, 1997.
[7] N. Mommer, M. Hirscher, F. Cuevas, H. Kronmüller, J. Alloys Comp. 266 (1998) 255.
[8] K. Yvon, W. Jeitschko, E. Parthé, J. Appl. Crystallography 20 (1977) 73.
[9] M. Ellner, U. Kattner, B. Predel, J. Less-Common Metals 87 (1982) 305.
[10] P. Villars, L.D. Calvert, Pearson's Handbook of Crystallographic Data for Intermetallic Phases, ASM International, The Materials Information Society, Materials Park, OH, 1991.
[11] E. Teatum, K. Gschneidner, J.M. Waber, (LA-2345 U.S. Department of Commerce, Washington, D.C. 1960), in: W.B. Pearson (Ed.), The Crystal Chemistry and Physics of Metals and Alloys, Wiley-Interscience, New York 1972, p. 151.
[12] C.E. Holley, R.N.R. Mulford, F.H. Ellinger, W.C. Koehler, W.H. Zachariasen, J. Phys. Chem 59 (1955) 1222.
[13] H. Müller, P. Knappe, O. Greis, Z. Phys. Chemie Neue Folge 114 (1979) 45.
[14] P. Knappe, H. Müller, Z. anorg. allg. Chem. 487 (1982) 63.
[15] K. Takemura, K. Syassen, J. Physics F: Metal Physics 15F (1985) 543.
[16] M. Mansmann, W.E. Walace, J. de Physique 25 (1964) 454.
[17] E. Parthé, L. Gelato, B. Chabot, M. Penzo, K. Cenzual, R. Gladyshevskii, TYPIX, Standardized Data and Crystal Chemical Characterization of Inorganic Structures, Vol. 4, Springer Verlag, Berlin 1994.
[18] R.M. Hazen, H.K. Mao, L.W. Finger, R.J. Hemley, Phys. Rev., B: Solid State 36B (1987) 3944.
[19] W.L. Korst, J.C. Warf, Inorganic Chemistry 5 (1966) 1719.
[20] T. Hahn (Ed.), International Tables for Crystallography, Volume A, Fourth, revised edition, Kluwer Academic Publishers, Dordrecht, 1996.
[21] B. Predel, Phasengleichgewichte, kristallographische und thermodynamische Daten binärer Legierungen, Band 5a, in Landolt-Börnstein, Neue Serie, Springer Verlag, Berlin, 1991.
[22] O. Knacke, O. Kubaschewski, K. Hesselmann, Thermochemical Properties of Inorganic Substances, Second Edition, Springer Verlag, Berlin, 1991.